TOXICOLOGICAL SCIENCES **108(1)**, 173–183 (2009)
doi:10.1093/toxsci/kfn222
Advance Access publication October 21, 2008

Inhalation Dosimetry of Diacetyl and Butyric Acid, Two Components of Butter Flavoring Vapors

John B. Morris*,[1] and Ann F. Hubbs†

*Toxicology Program, Department of Pharmaceutical Sciences, University of Connecticut, Storrs, Connecticut 06269; and †Pathology and Physiology Research Branch, Health Effects Laboratory Division, National Institute for Occupational Safety and Health, Centers for Disease Control and Prevention, Morgantown, West Virginia 26505

Received August 1, 2008; accepted October 11, 2008

Occupational exposure to butter flavoring vapors (BFV) is associated with significant pulmonary injury. The goal of the current study was to characterize inhalation dosimetric patterns of diacetyl and butyric acid, two components of BFV, and to develop a hybrid computational fluid dynamic-physiologically based pharmacokinetic model (CFD-PBPK) to describe these patterns. Uptake of diacetyl and butyric acid vapors, alone and in combination, was measured in the upper respiratory tract of anesthetized male Sprague-Dawley rats under constant velocity flow conditions and the uptake data were used to validate the CFD-PBPK model. Diacetyl vapor (100 or 300 ppm) was scrubbed from the airstream with 76–36% efficiency at flows of 100–400 ml/min. Butryic acid (30 ppm) was scrubbed with >90% efficiency. Concurrent exposure to butyric acid resulted in a small but significant reduction of diacetyl uptake (36 vs. 31%, $p < 0.05$). Diacetyl was metabolized in nasal tissues *in vitro*, likely by diacetyl reductase, an enzyme known to be inhibited by butyric acid. The CFD-PBPK model closely described diacetyl uptake; the reduction in diacetyl uptake by butyric acid could be explained by inhibition of diacetyl reductase. Extrapolation to the human via the model suggested that inspired diacetyl may penetrate to the intrapulmonary airways to a greater degree in the human than in the rat. Thus, based on dosimetric relationships, extrapulmonary airway injury in the rat may be predictive of intrapulmonary airway injury in humans. Butyric acid may modulate diacetyl toxicity by inhibiting its metabolism and/or altering its inhalation dosimetric patterns.

Key Words: **diacetyl; nose; inhalation; dosimetry.**

Fixed airways obstruction has been described in workers inhaling butter flavoring vapors (BFV) with morphologic changes including air trapping, bronchial wall thickening, and constrictive bronchiolitis (Akpinar-Elci *et al*., 2004; Kreiss *et al*., 2002). Short-term exposure of rats to BFV induces airway injury including necrosis and inflammation of the nasal passages, trachea, and bronchi (Hubbs *et al*., 2002). BFV are a complex mixture of volatile agents containing diacetyl (2,3-butanedione), acetoin, 2-nonanone, acetic acid, and butyric acid, among other vapors (Boylstein *et al*., 2006; Hubbs *et al*., 2002; Kullman *et al*., 2005). In both rats (Hubbs *et al*., 2008) and mice (Morgan *et al*., 2008), short-term exposure to 200 ppm or more of pure diacetyl results in severe nasal, tracheal, and bronchial injury providing evidence that diacetyl contributes significantly to the airway injury induced by BFV. Moreover, clinical bronchiolitis obliterans also affects workers manufacturing flavorings, including diacetyl (CDC, 2007; Kanwal, 2008; Van Rooy *et al*., 2007). Diacetyl is metabolized by diacetyl reductase (also known as dicarbonyl nicotine adenine dinucleotide phosphate reductase and dicarbonyl/L-xylose reductase; Nakagawa *et al*., 2002); this may represent a detoxification pathway. Butyric acid is a potent inhibitor of this enzyme, raising the possibility that a toxicological interaction may exist among components of BFV.

Regional deposition patterns of inspired materials are critical determinants of airway injury sites following inhalation exposure. Knowledge of inhalation deposition patterns is, therefore, essential for evaluating inhalation risk, particularly since regional dosimetry patterns may differ between rodents and humans (U.S. EPA, 1994). Scrubbing of vapors from the airstream is determined by the tissue:air partition coefficient, airway architecture and ventilation, and the ability of the airways to clear the vapor via the circulation and/or metabolism (Bogdanffy and Sarangapani, 2003; Dahl and Lewis, 1993; Morris, 1999a, 2006). Thus, e.g., inhibition of metabolic clearance pathways leads to a diminished scrubbing capacity (Morris, 1990, 1999b; Stanek and Morris, 1999). Mathematical dosimetry models have been developed to predict and understand nasal vapor dosimetry. Hybrid computational fluid dynamic-physiologically based pharmacokinetic models (CFD-PBPK), based on the approach developed in this laboratory (Morris *et al*., 1993), have been validated and used for assessment of a variety of vapors including acrylic acid

Disclaimer: The findings and conclusions in this report are those of the authors and do not necessarily represent the views of the National Institute for Occupational Safety and Health.

[1] To whom correspondence should be addressed at Department of Pharmaceutical Sciences, 69 North Eagleville Road, U-3092 University of Connecticut Storrs, CT 06269-3092. Fax: (860) 486-5792. E-mail: john.morris@uconn.edu.

(Frederick *et al*., 1998), ethyl acrylate (Frederick *et al*., 2002), vinyl acetate (Hinderliter *et al*., 2005; Plowchalk *et al*., 1997), acetaldehyde (Teeguarden *et al*., 2008), and acrolein (Schroeter *et al*., 2008).

The goal of the current study was to characterize nasal diacetyl dosimetry and its modulation by coexposure to butyric acid. Therefore, diacetyl and/or butyric acid uptake was measured in the surgically isolated upper respiratory tract (URT) of the rat at multiple flow rates covering the target concentration span used in rat inhalation toxicity studies (100–300 ppm; Hubbs *et al*., 2002, 2008). Diacetyl concentrations in butter flavor mixing rooms may approach 100 ppm, and concentrations in close proximity to the mixing vats are likely much higher (Kreiss *et al*., 2002). In addition, metabolism of diacetyl in nasal and lower extrapulmonary airways (trachea plus extrapulmonary main stem bronchi) was examined *in vitro*. From the uptake and metabolism data, a CFD-PBPK model for dosimetry of diacetyl was developed and validated. The model was then used to extrapolate the rat dosimetric relationships to the human.

MATERIALS AND METHODS

Animals and in vitro studies. All studies were performed on male Sprague-Dawley rats (Charles River, Wilmington MA, 7–12 weeks of age at time of use, average body weight 310 g). Uptake of vapors was measured in the isolated URT as described previously (Morris, 1999). Briefly, following the onset of anesthesia (urethane 1.3 g/kg ip) the trachea was incised and an endotracheal tube was inserted anteriorly until its tip lay at the larynx. The animal was placed in a nose-only chamber, and air was drawn through the URT at flow rates of 100, 200, or 400 ml/min for 1 h. The concentration of diacetyl was measured in chamber (inspired) air and in air exiting the isolated URT into the endotracheal tube. Uptake (as % inspired) was calculated from the ratio of the exiting to the inspired air concentration. Inspired air concentration was measured immediately before and after uptake measurement. (The ratio of the before and after samples averaged 97.5 ± 5.4%.) For *in vitro* studies, nasal respiratory and olfactory tissues were collected from nonexposed urethane-anesthetized rats and homogenized in 5 and 8 ml, respectively, of Krebs Ringer buffer in a Ten Broeck homogenizer. (The mass of the rat nasal mucosa in rats is approximately 100 mg; Casanova-Schmitz *et al*., 1984.) Animal protocols were approved by the University Institutional Animal Care and Use Committee.

Respiratory and olfactory homogenates (0.1 ml) were incubated with 1mM NADPH and 10mM diacetyl (total volume 1.0 ml), and the rate of oxidation of NADPH was monitored by absorbance at 340 nm for 10 min (Thermo Spectronic Genesis 10 Vis spectrophotometer, Madison, WI). Metabolism rates were linear with time and protein concentration. Air:water partition coefficient for diacetyl was determined by published methods (Morris and Cavanagh, 1986).

Exposures. Diacetyl and butyric acid atmospheres were generated by flash evaporation. Chamber air was heated and humidified (~38°C, water content >75% relative humidity [e.g., >30 mg/l]) to minimize nasal dehydration. Airborne concentrations were measured with Varian Model 3800 gas chromatograph equipped with a gas sampling valve, a 15M DB-WAX megabore column (Agilent Technologies, Santa Clara CA), and flame ionization detector detection. Air samples were injected onto the column every 3 or 5 min. For diacetyl, oven temperatures were 60°C. For butyric acid or diacetyl/butyric acid measurement, a temperature program was used: 60°C for 30 s followed by a ramp-up to 120°C (over 1 min) and a 2-min hold. Standard curves were prepared by volatilization of the materials in a glass flask and sampling through sampling valve.

Modeling. A CFD-PBPK model was developed using multiple tissue stacks lining the nasal and tracheal airways (Frederick *et al*., 1998; Morris *et al*., 1993; Teeguarden *et al*., 2008; see Fig. 1). An analogous structure was used for both the rat and the human model. The human model was run for two conditions, nose and mouth breathing. Since rats are obligate nose breathers, the rat model was run for only nose-breathing conditions. Each stack contained mucus, epithelial, and submucosal compartments. In the nose, airflow is split over a dorsal flow airstream which passes over a respiratory followed by an olfactory tissue stack. The ventral airstream passes over two equal-sized respiratory epithelial stacks (Morris *et al*., 1993; Teeguarden *et al*., 2008). The entire airstream passes over the trachea which was modeled with two equal-sized sequential stacks, representing the anterior and posterior trachea. Transfer of vapor from the air to the superficial mucus layer was modeled by the CFD approach of Frederick *et al*. (1998). The parameterization for the tissue stacks is described in the appendix. Model simulations were performed with ACSL software (Aegis Technologies, Huntsville, AL).

Statistical analysis. All calculations were performed with Statistica software. Values are expressed as mean ± SD. Data were compared by ANOVA, followed, as appropriate, by *post hoc* Newman-Keuls test. A $p < 0.05$ was required for significance.

RESULTS

In Vitro Studies

The water:air partition coefficient was measured by vial equilibration techniques at 37°C and averaged 550 ± 44. The reported *K*m for diacetyl metabolism is 1.1mM (Nakagawa *et al*., 2002). Initial studies revealed that this was a reasonable estimate for the *K*m for respiratory tissue metabolism. The specific activities for diacetyl metabolism as measured at an incubation concentration of 10mM are shown in Table 1. Activity was significantly higher in the nasal olfactory mucosa homogenate than in either the nasal or the tracheal respiratory mucosal homogenates.

Uptake Studies

URT uptake efficiency of diacetyl quickly achieved a plateau value during the 1-h exposure as indicated by constant exiting air concentrations (Fig. 2). As in previous studies (Morris, 1999a), the average value during the last 30 min of the exposure was used to represent the steady-state value.

The steady-state URT uptake efficiencies at all flow rates at 100 and 300 ppm are shown in Figure 3. Two-factor ANOVA revealed a significant effect of flow rate ($p < 0.0001$) with diminished uptake efficiencies being observed at the higher flow rates. Neither an effect of concentration ($p = 0.17$) nor an interaction between flow rate and concentration ($p = 0.33$) was detected. Also shown are the CFD-PBPK model (see below) predictions.

In a subsequent experiment, uptake efficiency of diacetyl alone (100 ppm), butyric acid alone (30 ppm), and the

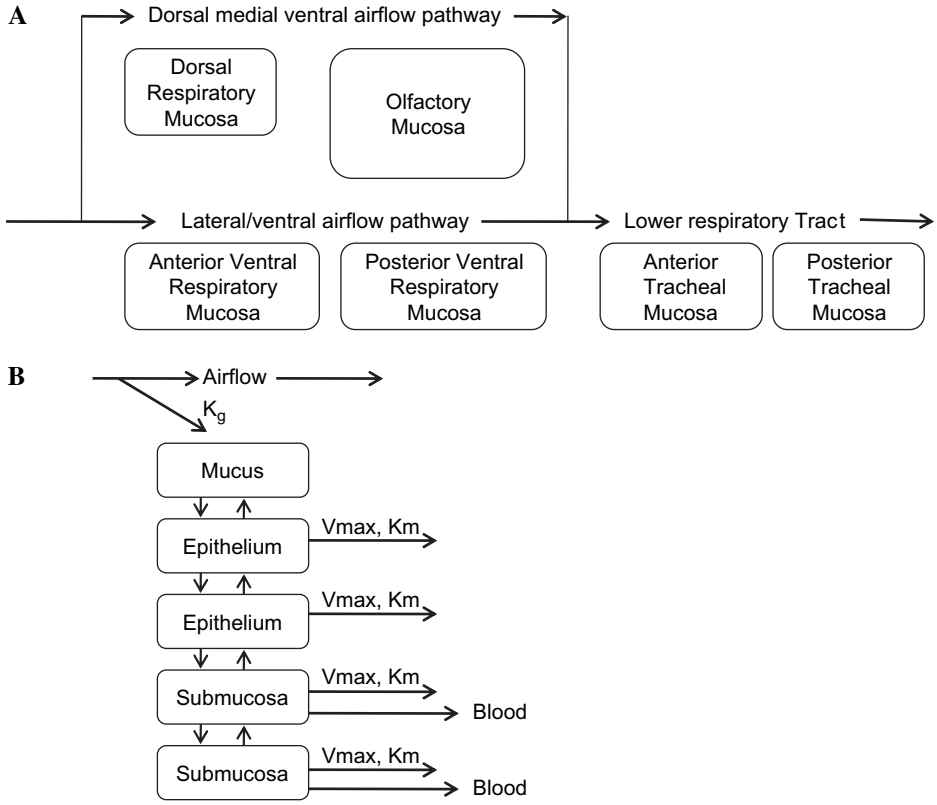

FIG. 1. (A) Schematic diagram of the airflow and mucosal types of CFD-PBPK model. In the nose, airflow splits into a dorsal medial airstream and a ventral airstream with 12 and 88% of flow, respectively (Kimbell *et al*., 1997; Morris *et al*., 1993), the two streams mix in the posterior nasal cavity, and a single stream flows over the tracheal mucosa. (B) Schematic of the tissue compartments in respiratory mucosal stacks. The respiratory mucosa of the nasal cavity and the mucosa of the trachea were modeled identically since both sites are lined with pseudostratified columnar mucociliated epithelium. The olfactory mucosa was modeled similarly except that it included four epithelial compartments to model the enhanced thickness of the epithelium in this mucosa. Vapor is transferred from air to the mucus lining layer in accordance with mass transport theory and described with an overall mass transport coefficient. Vapor can be metabolized in each tissue compartment by Michaelis-Menton kinetics. Vapor molecule is transferred between tissue compartments based on its estimated tissue diffusivity. Vapor in the submucosal compartments is assumed to be equilibrated with the blood perfusing those compartments.

combination were measured (Table 2). All measurements were made at a flow rate of 400 ml/min. This flow approximates the average inspiratory flow rate in the Sprague-Dawley rat (Teeguarden *et al*., 2008). Butyric acid was not detected in the air exiting the URT. Based on limits of detection, uptake efficiency exceeded 90%. Uptake of diacetyl was similar to that in the previous experiment (see Fig. 2). Diacetyl uptake was slightly but significantly reduced in animals exposed to the combined exposure to diacetyl and butyric acid ($p = 0.02$). A separate experiment revealed that uptake of acetone vapor was not influenced by concomitant exposure to butyric acid (data not shown), indicating that the effect of butyric acid was specific to diacetyl.

Model Simulations

The CFD-PBPK model was run with the metabolism data provided in Table 1 and a water:air partition coefficient of 550 as a surrogate for the mucus:air partition coefficient. There were no undefined variables that were fit to the diacetyl data. The model predictions for the three flow rates and two concentrations are shown in Figure 3. As can be seen, the predictions correlated strongly with the measured values, with the predictions being within one SD of the measured value. The model was used to predict uptake efficiencies in animals in which diacetyl reductase was inhibited by 0, 25, 50, 75, or 100%; predicted uptake efficiencies were 33, 32, 31, 29, and

TABLE 1
NADPH Metabolism of Diacetyl in Respiratory Tract Tissue Homogenates

	Specific activities (μmol/min per whole tissue)
Olfactory mucosa	1.0 ± 3 (10)
Respiratory mucosa	0.19 ± 0.06 (9)
Tracheal mucosa	0.13 ± 0.08 (5)

Note. Diacetyl metabolism was measured *in vitro* at a substrate concentration of 10mM. Preliminary studies revealed a *K*m of 1.1mM, similar to that reported previously (Nakagawa *et al*., 2002). Data represent the specific activities and are reported as mean ± SD (*n*).

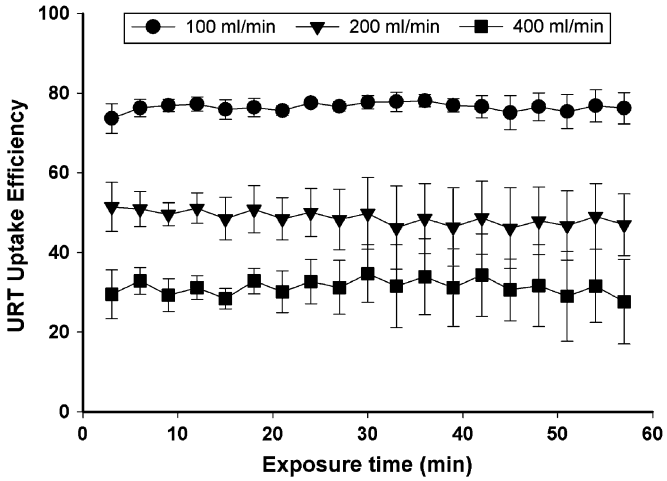

FIG. 2. Shown are the uptake efficiencies measured during the 1-h exposure to 100-ppm diacetyl at flow rates of 100 (circles), 200 (triangles), and 400 (squares) ml/min. Data are shown as mean ± SD. Repeated measures ANOVA did not detect a significant effect of time indicating that uptake efficiency remained constant throughout the entire 1-h exposure.

25%, respectively. Measured uptake efficiencies averaged 36 and 31% in diacetyl- and diacetyl/butyric acid–exposed animals (see Table 2). The modeling results, therefore, suggest that coexposure to butyric acid may have resulted in 50–75% inhibition of diacetyl reductase.

Shown in Table 3 are the CFD-PBPK model predictions for uptake efficiency as well as the predicted tissue concentrations of diacetyl in the superficial epithelial layers in the anterior and posterior ventral nose and the anterior and posterior superficial tracheal epithelium. These predictions are tabulated for the 400 ml/min flow rate because this flow approximates the average inspiratory flow rate in the Sprague-Dawley rat. Predicted tissue concentrations in respiratory epithelium were in the mM range and increased slightly more than linearly with inspired concentration. Predicted superficial olfactory epithelial concentrations were fourfold lower than those for the respiratory epithelium (data not shown). Predicted tracheal concentrations were fairly similar to those in the nasal respiratory epithelium. The model predicts that, like the URT, the trachea will also scrub diacetyl. A tracheal scrubbing efficiency of 7% is predicted at an inspired concentration of 100 ppm; the concentration of diacetyl in air exiting the trachea and entering the bronchi is predicted to be 61 ppm.

The regional nasal injury pattern following acute exposure to diacetyl has been characterized by Hubbs *et al*. (2008). In that study, four sections, T1, T2, T3, T4 (corresponding to the standard levels described by Young, 1981; see Hubbs *et al*., 2008), were taken through the nose of rodents exposed to 100- to 356-ppm diacetyl for 6 h in two separate experiments. T1

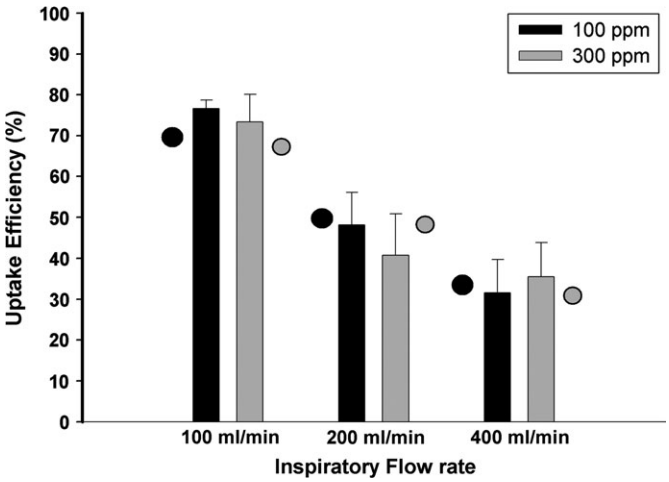

FIG. 3. Measured URT uptake efficiency for diacetyl at exposure concentrations of 100 or 300 ppm at flow rates of 100, 200, or 400 ml/min. Data are shown as mean ± SD. The closed and open circles represent model predictions for uptake efficiency at 100 and 300 ppm, respectively.

TABLE 2
Uptake of 100-ppm Diacetyl with and without Simultaneous 30-ppm Butryic Acid

	Measured uptake efficiencies (%)
Butyric acid (alone)	>90
Diacetyl (alone)	36.1 ± 3.7
Diacetyl with butyric acid	30.6 ± 3.5[a]

Note. Isolated URT uptake of butyric acid and/or diacetyl vapors was measured at an inspiratory flow rate of 400 ml/min. Data are reported as mean ± SD ($n = 6$).

[a]Significantly different than diacetyl alone ($p < 0.05$, *t*-test).

TABLE 3
CFD-PBPK Model Estimates for Tissue and Airborne Diacetyl Concentrations

	URT			Trachea		
	Anterior ventral mucosa (mM)	Posterior ventral mucosa (mM)	Exiting air (ppm)	Anterior tracheal mucosa (mM)	Posterior tracheal mucosa (mM)	Exiting air (ppm)
RAT						
100 ppm	1.6	1.4	67	1.2	1.1	61
200 ppm	3.2	2.8	136	2.5	2.4	125
300 ppm	4.9	4.2	206	3.8	3.7	191
Human—100 ppm						
Nose	1.4	1.2	82	1.2	1.2	79
Mouth	—	—	—	1.5	1.5	96

Note. Model predictions for tissue or air diacetyl concentrations in rats or humans at flow rates of 400 and 13,890 ml/min, respectively. Data are presented to two significant figures for the sake of clarity. It should not be inferred that the predictions are accurate to this degree.

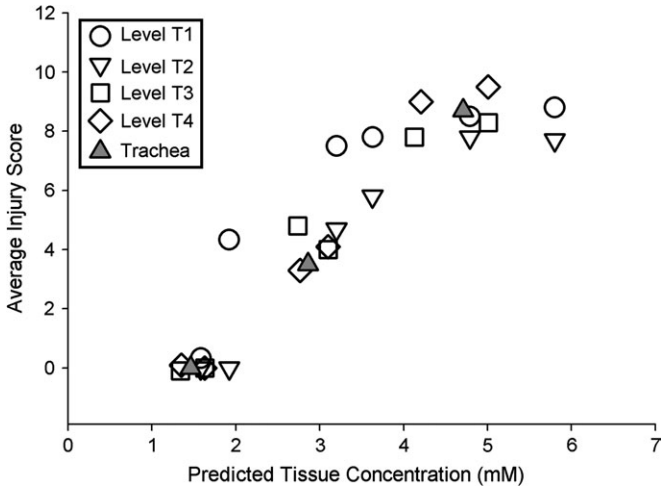

FIG. 4. The average pathology scores for rats exposed to 100-, 200-, or 300-ppm diacetyl for 6 h from Hubbs *et al.* (2008) are plotted versus the CFD-PBPK model–predicted tissue concentrations at these exposure levels. Included are data from all sections of the nose (T1–T4) and all exposure concentrations.

and T2 correspond to the anterior respiratory mucosal stacks and T3 and T4 to the posterior respiratory mucosal stacks of the CFD-PBPK model. Shown in Figure 4 are the average acute pathology scores plotted against the predicted tissue concentrations from Table 3. All levels from all exposure concentrations were included in this figure. As can be seen, a strong correlation between injury and predicted tissue concentrations was observed for the nasal tissues. Acute injury was generally apparent only in tissue in which predicted concentrations exceeded 2mM. Diacetyl exposure also results in tracheal injury; values for the trachea are also included in the plot and appear to fall within the same relationships observed for the nasal tissues.

The CFD-PBPK model can be scaled to predict uptake efficiencies and tissue concentrations in the human by using anatomic parameters (surface areas, blood flows, etc.) and air-phase mass transfer coefficients for the human (Frederick *et al.*, 1998; Teeguarden *et al.*, 2008). Diacetyl metabolism rates in airway mucosa of the human are not known but were assumed to be identical to those of the rat on a surface area basis (see appendix). The model predicts that at average inspiratory flow rates (13.8 l/min) the human nose and trachea will scrub diacetyl with 18 and 3% efficiency, values considerably lower than the rat (see above). In nose-breathing humans inhaling 100-ppm diacetyl, it is estimated that concentrations of diacetyl in air exiting the trachea will be 79 ppm. In mouth-breathing humans, tracheal exiting air concentrations of 96 ppm are predicted. These values are higher than the 61 ppm predicted for the nose-breathing rat. Predicted nasal and tracheal tissue concentrations are similar to those in the rat.

Sensitivity analysis of model predictions provides insights into those factors which strongly influence inhalation dosimetry. The sensitivity analysis was based on the predicted URT uptake efficiency because this was the experimentally measured parameter. For this analysis, each individual parameter was changed by 10% from its original value and the resulting change in predicted uptake efficiency was calculated. Thus, a 10% proportional change in uptake efficiency would represent a 1:1 sensitivity with the parameter of interest. Shown in Table 4 are the results obtained for key parameters including partition coefficient, mass transfer coefficient, tissue depth, metabolism rate, and perfusion rate. In the rat, predicted uptake efficiency was most sensitive to partition coefficient, tissue depth, vapor tissue diffusivity, and tissue perfusion rate. Uptake efficiency was modestly sensitive to metabolic V_{max} and insensitive to the mass transfer coefficient. Reducing the mass transfer coefficient 10-fold resulted in only a 1% decrease in predicted uptake efficiency. Sensitivity analysis for human URT uptake produced similar results. In the human, uptake was also most strongly sensitive to partition coefficient, tissue depth, tissue vapor diffusivity, and blood flow. Although the absolute value was low, the human uptake predictions were considerably more sensitive than the rat to changes in the air-phase mass transfer coefficient. Lowering the mass transfer coefficient by 10-fold resulted in a 38% reduction in predicted uptake efficiency compared to only a 1% reduction for the rat.

TABLE 4
Sensitivity Analysis: Percent Change in Predicted URT Exiting Air Concentration Caused by a 10% Change in Each Identified Parameter

	Rat (%)	Human (%)
Air-phase mass transfer coefficient	+0.004	+0.8
Partition coefficient	+5.7	+7.2
Tissue compartment depth	−3.6	−5.7
Tissue diffusivity	+2.9	+5.8
Metabolism rate—V_{max}		
Respiratory mucosa	+0.9	+0.7
Olfactory mucosa	+0.3	+0.3
Tissue blood flow	+2.4	+1.4

Note. Shown is the percent change in URT uptake efficiency caused by a 10% change in each parameter; e.g., if uptake efficiency was increased from 30 to 33% this would be reported as a 10% increase. A positive sign indicates that uptake efficiency was decreased by decreasing the parameter of interest; a negative sign indicates that uptake efficiency was increased. Sensitivity analyses were performed at a flow rate approximating the average inspiratory flow rate (400 and 13,890 ml/min in the rat and human) and an inspired concentration of 100 ppm.

DISCUSSION

Acute exposure to diacetyl results in injury in the nasal passages and large airways of the rat (Hubbs *et al.*, 2008).

Inhalation dosimetric patterns are often critical in influencing the site of injury to inspired materials (U.S. EPA, 1994). The current study characterizes the upper airway dosimetry of diacetyl from both an experimental (uptake efficiency measurement) and a theoretical (CFD-PBPK modeling) perspective. Uptake of vapor in the airways is determined by the balance of delivery to the airway walls from the airstream and clearance from tissues via the bloodstream, metabolism, and/or direct reactivity. The potential importance of metabolism in influencing uptake has been shown by numerous studies which document that pretreatment with xenobiotic metabolizing enzyme inhibitors diminishes uptake efficiencies (Morris, 1990, 1999; Stanek and Morris, 1999). In general, vapors that partition extensively into tissue and/or are reactive or quickly metabolized are scrubbed from the upper airways with high efficiency. For example, weak acids (hydrofluoric, acetic, acrylic acid) are soluble and reactive in that they ionize at physiological pH. Nasal uptake efficiencies in excess of 95% are observed for such vapors (Morris and Frederick, 1995; Morris and Smith, 1982; Vaughan *et al*., 2006). In the current study, URT uptake efficiency in excess of 90% was observed for butyric acid, a result fully consistent with the existing database. Modern modeling approaches, including hybrid CFD-PBPK models, have successfully captured uptake behavior of metabolized and/or reactive vapors and have been useful in defining and extrapolating dosimetric relationships in the rat and human.

The current studies reveal that diacetyl is a ''soluble'' vapor as indicated by a water:air partition coefficient (W/A) of 550; a partition coefficient that is higher than acetone and lower than ethanol vapor (Morris and Cavanagh, 1986). Based on its partition coefficient, moderate (e.g., 25–75%) URT uptake efficiencies would be expected for diacetyl; such efficiencies were observed. Scrubbing of vapors in the nose is an important respiratory defense mechanism in that it serves to protect the lower airways. Rats are obligate nose breathers; thus, in rats the concentration of airborne vapor reaching the lungs is often much lower than the ambient air concentration. This is also true in the nose-breathing human, but during mouth breathing this defense mechanism is lost. Thus, a challenge in interpreting inhalation toxicity data is extrapolating responses in nose-breathing rodents to mouth-breathing humans.

Diacetyl was found to be metabolized in nasal and tracheal tissues via a NADPH-dependent pathway, presumably diacetyl reductase. This enzyme has previously been shown to be present in airways of the rodent and human (Nakagawa *et al*., 2002); thus, its detection in nasal tissues is not unexpected. Specific activity was approximately fourfold higher in olfactory than nasal respiratory or tracheal tissues (Table 3). This is a common pattern for nasal enzymology (Dahl and Hadley, 1991). This enzyme is thought to be a detoxification pathway for diacetyl (Nakagawa *et al*., 2002). Butyric acid is a potent inhibitor of diacetyl reductase (Nakagawa *et al*., 2002). By analogy to numerous previous studies (Morris, 1990, 1999; Stanek and Morris, 1999), inhibition of nasal metabolism of diacetyl should result in decreased scrubbing capacity. The current results indicate that coexposure to butyric acid significantly reduces nasal uptake efficiency of diacetyl but not acetone vapor. The absence of effect on acetone vapor uptake suggests that butyric acid (at this exposure level) does not cause nasal vasodilation and increased blood flow (Morris *et al*., 1999). The significance of this result is threefold. First, this provides evidence that inspired diacetyl is indeed metabolized in the nasal tissues via a butyric acid–sensitive pathway, likely diacetyl reductase. Second, reduced nasal scrubbing capacity of diacetyl vapors in the presence of butyric acid or other diacetyl reductase inhibitors will enhance more distal penetration of inspired diacetyl and, therefore, places the lower airways at greater risk. Third, if diacetyl reductase is a detoxification pathway, by inhibiting this enzyme, butyric acid would enhance the toxicity of diacetyl in those tissues in which both vapors deposit. Since butyric acid is scrubbed with high efficiency in the nose, this interaction most likely occurs in the nasal airways of the rat. Under mouth-breathing conditions, the same phenomenon would be anticipated in the large airways of humans.

The uptake efficiency observed in the rat during coexposure to diacetyl and butyric acid was consistent with a butyric acid–induced 75% reduction in metabolic capacity. This may reflect a 75% inhibition diffusely throughout the nasal airways. Alternatively, and more likely, this represents the deposition patterns of butyric acid. As evidenced by strong anterior-posterior gradients in nasal injury by weak acids (Buckley *et al*., 1984; Rosenholtz *et al*., 1963) in the rat, butyric acid likely only deposits most heavily in the anterior portions of the nose; thus, a greater degree of inhibition would be expected in the anterior than posterior nasal regions, and any inhibition of nasal diacetyl reductase in the rat may have been focal in nature. Irrespective of the focal versus diffuse nature of any inhibition, these studies indicate that there is a dosimetric interaction among the components of BFV and highlight the need to consider the multiple components of BFV in comprehensive safety evaluations. Our study utilized a butyric acid concentration which was 30% of the diacetyl concentration. This concentration was necessary to demonstrate inhibition of the butyric acid–sensitive diacetyl metabolic pathway in the nose, which is presumed to be diacetyl reductase. While butyric acid is a common vapor in microwave popcorn production (Boylstein *et al*., 2006) and the most powerful known inhibitor of diacetyl reductase (Nakagawa *et al*., 2002), its relative concentration to diacetyl in workplaces is incompletely investigated at this time.

Computational modeling has proved very useful in understanding and extrapolating inhalation dosimetry patterns for diverse vapors such as acrylic acid (Frederick *et al*.,

1998), ethyl acrylate (Frederick *et al.*, 2002), acetaldehyde (Teeguarden *et al.*, 2008), and acrolein (Schroeter *et al.*, 2008). In the current study, this modeling approach closely predicted URT uptake efficiencies of diacetyl. It is important to note that the model was not fit to the diacetyl data, rather the model was applied simply by inputting the diacetyl-specific data. Nasal injury patterns from inspired vapors are often highly localized; dosimetry models have provided data implicating regional dosage rates as being a key contributor to regionalized injury (Kimbell *et al.*, 1997; Schroeter *et al.*, 2006, 2008). Using an approach conceptualized by Kimbell (Kimbell *et al.*, 1997), the regional nasal injury scores in diacetyl-exposed rats were correlated with the predicted regional tissue concentrations within the nose. A strong correlation was seen. These data suggest that acute epithelial injury results when tissue concentrations exceed 2mM. The strong correlation enhances confidence in the model predictions and suggests that, as for other vapors (Kimbell *et al.*, 1997; Schroeter *et al.*, 2006, 2008), regional dosage rates are important determinants of regional nasal injury following acute diacetyl exposure. One limitation of the model predictions is that they are made assuming constant velocity unidirectional flow rather than cyclic breathing. However, it is thought that predictions under these constant velocity flow conditions are reflective of dosimetry patterns under normal respiration (Andersen and Sarangapani, 1999).

An additional limitation is that our study does not model the effect of subchronic or chronic exposure to diacetyl. In mice, a 12-week exposure to 100-ppm diacetyl produces denudation, atrophy, and regeneration of bronchial epithelium with lymphocytic bronchitis seen at lower exposures, effects that may well occur when tissue concentrations are less than 2mM. It is for this reason that the 2mM value discussed in this publication should not be used for assessment of risks associated with chronic exposure scenarios. Our study does suggest the potential importance of changes seen in the nose during subchronic exposures that might affect nasal uptake of diacetyl, including chronic inflammation, squamous metaplasia, respiratory metaplasia of olfactory epithelium, and olfactory epithelial atrophy (Morgan *et al.*, 2008). CFD-PBPK modeling of subchronic and chronic low-level effects is a future research need. It should also be noted that measurement of URT uptake efficiencies and validation of the model for lower exposure concentrations would also represent a future research need.

In rodents, diacetyl also induces injury in the trachea and bronchi (Hubbs *et al.*, 2008, Morgan *et al.*, 2008). Both the nasal cavity and large airways are lined with a pseudostratified columnar mucociliated epithelium, but it is not known if these tissues are of equal sensitivity to diacetyl. To assess this issue, the CFD-PBPK model structure was used to extrapolate tissue concentrations in the trachea. Because there are no measures of tracheal uptake, these represent extrapolations. Extrapolated tracheal diacetyl concentrations exceed 2mM in animals exposed to 200 ppm or higher but not 100 ppm. Injury in the lower airways was not observed at the 100-ppm exposure level but was observed in rats exposed to 200 ppm and higher concentrations. Perhaps, more revealing is the relationship between the degree of tracheal injury versus the predicted tracheal epithelial concentration. These values for the trachea fell entirely within the ranges of values observed for the nasal epithelium (see Fig. 4). This provides suggestive evidence that the respiratory epithelium of the nose and trachea is of similar sensitivity to diacetyl-induced injury.

The hybrid CFD-PBPK modeling approach was developed to facilitate rodent-to-man extrapolations (Frederick *et al.*, 1998). This is accomplished by using the human-specific parameters in the model. This approach was used to predict nasal uptake efficiencies for vinyl acetate which were subsequently confirmed by experimentation (Hinderliter *et al.*, 2005). Because there is a strong scientific foundation for these models, the output represents informed estimates of human inhalation dosimetric relationships. The model predicts that diacetyl will be scrubbed with less efficiency in the upper airways in the human than in the rodent. In this regard, diacetyl appears similar to acrylic acid, vinyl acetate, and ethyl acrylate (Frederick *et al.*, 1998, 2002; Hinderliter *et al.*, 2005). From an inhalation risk perspective, reduced scrubbing capacity in the upper airways of the human correlates with increased delivery of material to potentially more sensitive lower airway sites.

The sensitivity analysis of the CFD-PBPK provides insights into important pathways for diacetyl uptake. In general terms, in both the rat and the human uptake efficiency was moderately dependent on metabolism rate (as measured by V_{max}) and more strongly sensitive to partition coefficient, tissue depth, tissue vapor diffusivity, and blood flow rates. These observations suggest that partitioning into tissue and removal via the circulation is the predominant pathway responsible for diacetyl uptake. Since the depth of the nasal mucosa in the human is greater than in the rat, uptake via this pathway in the human would be expected to be less effective than in the rat. This may be the primary basis for the lower predicted uptake efficiency in the human. URT uptake efficiency in the human appears to be more sensitive than in the rat to the partition coefficient, tissue diffusivity, and tissue depth; similar observations have been made in modeling efforts on acrolein (Schroeter *et al.*, 2008) but not acetaldehyde (Teeguarden *et al.*, 2008). Thus, these relationships may be vapor specific. Predicted URT uptake efficiency in the rat was insensitive to changes in the air-phase mass transfer coefficient suggesting that a minimal air-phase diffusion limitation exists in this species. Previous modeling efforts have reached a similar conclusion (Bush *et al.*, 1998; Frederick *et al.*, 1998). Although on an absolute basis human nasal cavity uptake was not particularly

sensitive to air-phase mass transfer coefficient, it was considerably more sensitive than the rat. This is particularly evident when comparing the effect of reducing the mass transfer coefficient by 10-fold. This produced less than a 1% change in predicted diacetyl uptake in the rat compared to a 30% reduction in the human, results very similar to those for acrylic acid vapor (Frederick *et al*., 1998). *In toto*, these results suggest that there is a proportionately greater air-phase resistance to uptake in the human than in the rat URT.

Clinical findings in individuals occupationally exposed to high concentrations of BFV indicate bronchiolar injury, data supported by the presence of constrictive bronchiolitis in two of the three patients with lung biopsies (Akpinar-Elci *et al*., 2004). However, nasal and tracheal/bronchial injury predominates in rodents exposed to BFV or diacetyl (Akpinar-Elci *et al*., 2004; Hubbs *et al*., 2002, 2008; Kreiss *et al*., 2002; Van Rooy *et al*., 2007). This species difference in regional respiratory tract injury is not uncommon. For example, hydrogen fluoride has long been known to be a lower respiratory tract irritant in the human (Dalbey *et al*., 1998), yet in the rodent it is scrubbed with high efficiency in the nose and produces injury only in that site (Dalbey *et al*., 1998; Morris and Smith, 1982; Rosenholtz *et al*., 1963; Stavert *et al*., 1991). Formaldehyde injury and DNA-protein cross-link levels are elevated in the anterior portion of the nose of rodents but are observed in the trachea and major bronchi as well as the nose in the monkey; decreased scrubbing capacity of the upper airways of the primate compared to the rodent is thought to be a critical factor in this species difference (Casanova *et al*., 1991).

The current model projects less-efficient airway scrubbing of diacetyl in the nose-breathing human than in the rat. It is important to recognize that in mouth-breathing humans, the nasal passages are bypassed and delivery to the lower airways is enhanced over that in nose breathing. The concentration of diacetyl in air penetrating to the bronchi in nose-breathing rats exposed to 100 ppm was predicted to be 62 ppm; in contrast, in mouth-breathing humans this concentration was predicted to be 97 ppm, roughly 1.5-fold higher, suggesting that the delivered dose to intrapulmonary airways in the human may be much greater than that in the rat. In addition to these factors, the dosimetric interaction between diacetyl and butyric acid may also be important in regional airway injury in humans exposed to butter flavor vapors. The current results indicate that butyric acid diminishes upper airway scrubbing of diacetyl and enhances its penetration to the lower airways. This was shown for the nose but would likely also occur in the large airways during mouth breathing. Thus, on the basis of these dosimetric relationships, it would appear that nasal and tracheal airway injury in the rodent exposed to diacetyl may well be predictive of injury in the intrapulmonary airways of mouth-breathing humans exposed to airborne BFV.

FUNDING

The National Institutes of Health (ES014041).

ACKNOWLEDGMENTS

The authors thank Barbro Simmons for her expert technical assistance and Daniel Willis for his helpful comments and suggestions.

REFERENCES

Akpinar-Elci, M., Travis, W. D., Lynch, D. A., and Kreiss, K. (2004). Bronchiolitis obliterans syndrome in popcorn production plant workers. *Eur. Respir. J.* **24,** 298–302.

Andersen, M. E., and Sarangapani, R. (1999). Clearance concepts applied to the metabolism of inhaled vapors in tissues lining the nasal cavity. *Inhal. Toxicol.* **11,** 873–897.

Bogdanffy, M. S., and Sarangapani, R. (2003). Physiologically-based kinetic modeling of vapours toxic to the respiratory tract. *Toxicol. Lett.* **128,** 103–117.

Boylstein, R., Piacitelli, C., Grote, A., Kanwal, R., Kullman, G., and Kreiss, K. (2006). Diacetyl emissions and airborne dust from butter flavoring used in microwave popcorn production. *J. Occup. Environ. Hyg.* **3,** 530–535.

Buckley, L. A., Jiang, X. Z., James, R. A., Morgan, K. T., and Barrow, C. S. (1984). Respiratory tract lesions induced by sensory irritants at the RD50 concentration. *Toxicol. Appl. Pharmacol.* **74,** 417–429.

Bush, M. L., Frederick, C. B., Kimbell, J. S., and Ultman, J. S. (1998). A CFD-PBPK hybrid model for simulating gas and vapor uptake in the rat nose. *Toxicol. Appl. Pharmacol.* **150,** 133–145.

Casanova, M., Morgan, K. T., Steinhagen, W. H., Everitt, J. I., Popp, J. A., and Heck, H. D. (1991). Covalent binding of inhaled formaldehyde to DNA in the respiratory tract of rhesus monkeys: pharmacokinetics, rat-to-monkey interspecies scaling and extrapolation to man. *Fundam. Appl. Toxicol.* **17,** 409–428.

Casanova-Schmitz, M., David, R. M., and Heck, H. D. (1984). Oxidation of formaldehyde and acetaldehyde by NAD+-dependent dehydrogenases in rat nasal mucosal homogenates. *Biochem. Pharmacol.* **33,** 1137–1142.

Centers for Disease Control and Prevention (CDC). (2007). Fixed obstructive lung disease among workers in the flavor manufacturing industry—California, 2004–2007. *MMWR Morb. Mortal. Wkly. Rep.* **56,** 389–393.

Condorelli, P., and George, S. C. (1999). Theoretical gas phase mass transfer coefficients for endogenous gases in the lungs. *Ann. Biomed. Eng.* **27,** 326–339.

Dahl, A. R., and Hadley, W. M. (1991). Nasal cavity enzyme involved in xenobiotic metabolism: effects on the toxicity of inhalants. *Crit. Rev. Toxicol.* **21,** 345–372.

Dahl, A. R., and Lewis, J. L. (1993). Respiratory tract uptake of inhalants and metabolism of xenobiotics. *Annu. Rev. Pharmacol. Toxicol.* **33,** 383–407.

Dalbey, W., Dunn, B., Bannister, R., Daughtrey, W., Kivwin, C., Reigman, K. F., Steiner, A., and Bruce, J. (1998). Acute effects of 10-minute exposure to hydrogen fluoride in rats and derivation of a short-term exposure limit for humans. *Regul. Toxicol. Pharmacol.* **27,** 207–216.

Frederick, C. B., Bush, M. L., Lomax, L. B., Black, K. A., Finch, L., Kimbell, J. S., Morgan, K. T., Subramaniam, R. P., Morris, J. B., and Ultman, J. S. (1998). Application of a hybrid computational fluid dynamics and physiologically based inhalation model for interspecies dosimetry

extrapolation of acidic vapors in the upper airways. *Toxicol. Appl. Pharmacol.* **152,** 211–231.

Frederick, C. B., Lomax, L. G., Black, K. A., Finch, L., Scribner, H. E., Kimbell, J. S., Morgan, K. T., Subramaniam, R. P., and Morris, J. B. (2002). Use of a hybrid computational fluid dynamics and physiologically based inhalation model for interspecies dosimetry comparisons of ester vapors. *Toxicol. Appl. Pharmacol.* **183,** 23–40.

Hinderliter, P. M., Thrall, K. D., Corley, R. A., Blemen, L. J., and Bogdanffy, M. S. (2005). Validation of human physiologically based pharmacokinetic model for vinyl acetate against human nasal dosimetry data. *Toxicol. Sci.* **85,** 460–467.

Hubbs, A. F., Battelli, L. A., Goldsmith, W. T., Porter, D. W., Frazer, D., Friend, S., Schwegler-Berry, D., Mercer, R. R., Reynolds, J. S., Grote, A., *et al.* (2002). Necrosis of nasal and airway epithelium in rats inhaling vapors of artificial butter flavoring. *Toxicol. Appl. Pharmacol.* **185,** 128–135.

Hubbs, A. F., Goldsmith, W. T., Kashon, M. L., Frazer, D., Mercer, R. R., Battelli, L. A., Kullman, G. J., Schwegler-Berry, D., Friend, S., and Castranova, V. (2008). Respiratory toxicologic pathology of inhaled diacetyl in Sprague-Dawley rats. *Toxicol. Pathol.* **36,** 330–344.

Kanwal, R. (2008). Bronchiolitis obliterans in workers exposed to flavoring chemicals. *Curr. Opin. Pulm. Med.* **14,** 141–146.

Kimbell, J. S., Gross, E. A., Richardson, R. B., Conolly, R. B., and Morgan, K. T. (1997). Correlation of regional formaldehyde flux predictions with the distribution of formaldehyde-induced squamous metaplasia in F344 rat nasal passages. *Mutat. Res.* **380,** 143–154.

Kreiss, K., Gomaa, A., Kullman, G., Fedan, K., Simoes, E. J., and Enright, P. L. (2002). Clinical bronchiolitis obliterans in workers at a microwave-popcorn plant. *N. Engl. J. Med.* **347,** 330–338.

Kullman, G., Boylstein, R., Jones, W., Piacitelli, C., Pendergrass, A., and Kreiss, K. (2005). Characterization of respiratory exposures at a microwave popcorn plant with cases of bronchiolitis obliterans. *J. Occup. Environ. Hyg.* **2,** 169–178.

Mahmood, U., Ridgeway, J., Jackson, R., Guo, S., Su, J., Armstrong, W., Shibuya, T., Crumley, R., Chen, Z., and Wong, B. (2006). *In vivo* optical coherence tomography of the nasal mucosa. *Am. J. Rhinol.* **20,** 155–159.

Mariassy, A. T. (1992). Epithelial cells of trachea and bronchi. In *Comparative Biology of the Normal Lung* (R. A. Parent, Ed.), pp. 63–76. CRC Press, Boca Raton, FL.

Martin, A., Swarbrick, J., and Cammarate, A. (1983). In *Physical Pharmacy: Physical Chemical Principles in the Pharmaceutical Sciences*. Lea & Fegiber, Philadelphia, PA.

McBride, J. (1992). Architecture of the tracheobronchial tree. In *Comparative Biology of the Normal Lung* (R. A. Parent, Ed.), pp. 49–61. CRC Press, Boca Raton, FL.

Morgan, D. L., Flake, G. P., Kirby, P. J., and Palmer, S. M. (2008). Respiratory toxicity of diacetyl in C57BL/6 mice. *Toxicol. Sci.* **103,** 169–180.

Morris, J. B. (1990). First-pass metabolism of inspired ethyl acetate in the upper respiratory tracts of the F344 rat and syrian hamster. *Toxicol. Appl. Pharmacol.* **102,** 331–345.

Morris, J. B. (1999a). A method for measuring upper respiratory tract vapor uptake and its applicability to quantitative inhalation risk assessment. *Inhal. Toxicol.* **11,** 101–123.

Morris, J. B. (1999b). Uptake of styrene vapor in the upper respiratory tracts of the CD mouse and Sprague-Dawley rat. *Toxicol. Sci.* **54,** 222–228.

Morris, J. B. (2006). Nasal toxicology. In *Inhalation Toxicology: Research Methods, Applications and Evaluation*, 2nd ed. (H. Salem, Ed.), pp. 349–371. Taylor and Francis, Boca Raton, FL.

Morris, J. B., and Cavanagh, D. G. (1986). Deposition of ethanol and acetone vapors in the upper respiratory tract of the rat. *Fundam. Appl. Toxicol.* **6,** 78–88.

Morris, J. B., and Frederick, C. B. (1995). Upper respiratory tract uptake of acrylate ester and acid vapors. *Inhal. Toxicol.* **7,** 557–574.

Morris, J. B., Hassett, D. N., and Blanchard, K. T. (1993). A physiologically based pharmacokinetic model for nasal uptake and metabolism of non-reactive vapors. *Toxicol. Appl. Pharmacol.* **123,** 120–129.

Morris, J. B., and Smith, F. A. (1982). Regional deposition and absorption of inhaled hydrogen fluoride in the rat. *Toxicol. Appl. Pharmacol.* **62,** 81–89.

Morris, J. B., Stanek, J., and Gianutsos, G. (1999). Sensory nerve-mediated immediate nasal responses to inspired acrolein. *J. Appl. Physiol.* **87,** 1877–1886.

Nakagawa, J., Ishikura, S., Asami, J., Isajii, T., Usami, N., Hara, A., Sakurai, T., Tsuritani, K., Oda, K., Takahashi, M., *et al.* (2002). Molecular characterization of mammalian dicarbonyl/L-xylulose reductase and its localization in kidney. *J. Biol. Chem.* **277,** 17883–17891.

Plowchalk, D. R., Andersen, M. E., and Bogdanffy, M. S. (1997). Physiologically based modeling of vinyl acetate uptake, metabolism, and intracellular pH changes in the rat nasal cavity. *Toxicol. Appl. Pharmacol.* **142,** 386–400.

Rosenholtz, M. J., Carson, T. R., Weeks, M. H., Wilinski, F., Ford, D. F., and Oberst, F. W. (1963). A toxicopathological study in animals after brief single exposures to hydrogen fluoride. *Am. Ind. Hyg. Assoc. J.* **24,** 253–261.

Schroeter, J. D., Kimbell, J. S., Andersen, M. E., and Dorman, D. C. (2006). Use of pharmacokinetic-driven computational fluid dynamics model to predict nasal extraction of hydrogen sulfide in rats and humans. *Toxicol. Sci.* **94,** 359–367.

Schroeter, J. D., Kimbell, J. S., Gross, E. A., Willson, G. A., Dorman, D. C., Tan, Y.-M., and Clewell, H. J. (2008). Application of physiological computational fluid dynamics models to precit interspecies nasal dosimetry of inhaled acrolein. *Inhal. Toxicol.* **20,** 227–243.

Stanek, J. J., and Morris, J. B. (1999). The effect of inhibition of aldehyde dehydrogenase on nasal uptake of inspired acetaldehyde. *Toxicol. Sci.* **49,** 225–231.

Stavert, D. M., Archuleta, D. A., Behr, M. J., and Lehnert, B. E. (1991). Relative acute toxicities of hydrogen fluoride, hydrogen chloride and hydrogen bromide in nose- and pseudo-mouth-breathing rats. *Fundam. Appl. Toxicol.* **16,** 636–655.

Teeguarden, J. G., Bogdanffy, M. S., Covington, T. R., Tan, C., and Jarabek, A. M. (2008). A PBPK model for evaluating the impact of acetaldehyde dehydrogenase polymorphisms on comparative rat and human nasal tissue acetaldehyde dosimetry. *Inhal. Toxicol.* **20,** 375–390.

United States Environmental Protection Agency. (1994). *Methods for Derivation of Inhalation Reference Concentrations and Application of Inhalation Dosimetry*. Office of Health and Environmental Assessment, Washington, DC.

Van Rooy, G. B. G. J., Rooyackers, J. M., Prokop, M., Houba, R., Smit, L. A. M., and Heederik, D. J. J. (2007). Bronchiolitis obliterans syndrome in chemical workers producing diacetyl for food flavorings. *Am. J. Respir. Crit. Care Med.* **176,** 498–504.

Van Winkle, L. S., Fanucchi, M. V., Miller, L. A., Baker, G. L., Gershwin, L. J., Schlegle, E. S., Hyde, D. M., Evans, J. M., and Plopper, C. G. (2004). Epithelial cell distribution and abundance in rhesus monkey airways during postnatal lung growth and development. *J. Appl. Physiol.* **97,** 2355–2363.

Vaughan, R. P., Szewczyk, M. T., Lanosa, M. J., DeSesa, C. R., Gianutsos, G., and Morris, J. B. (2006). Adenosine sensory transduction pathways contribute to activation of the sensory irritation response to inspired irritant vapors. *Toxicol. Sci.* **93,** 411–421.

Young, J. T. (1981). Histopathologic examination of the rat nasal cavity. *Fundam. Appl. Toxicol.* **1,** 309–312.

APPENDIX

Simulation Modeling

The hybrid CFD-PBPK model for diacetyl dosimetry was based on the PBPK approach developed in this laboratory (Morris *et al.*, 1993) incorporating the CFD components described by Frederick *et al.* (1998) and uses essentially the same as the model structure as Teeguarden *et al.* (2008). This general structure is shown in Figure 1. This structure has been widely used and validated for a variety of vapors (see text). A listing of select model parameters is provided in Table A1, and the values of the remaining parameters are provided in Morris *et al.* (1993).

The model consists of a moving airstream that passes over respiratory tissues that are modeled as stacks of tissue, the dimensions of which are anatomically defined. Based on the modeling efforts of Kimbell *et al.* (1997), the nasal airstream is partitioned into two flow streams in the nose, a dorsal flow path which passes over the dorsal medial meatus (modeled as the dorsal respiratory mucosal stack) and then over the ethmoturbinates (modeled as the olfactory mucosal stack). Flow through this stream constitutes 12% of the total nasal airflow (Morris *et al.*, 1993). The ventral flow pathway (88% of total nasal airflow) passes over two sequential respiratory mucosal tissue stacks (anterior ventral and posterior ventral). The two streams were mixed, and the entire airstream then passes over the trachea, modeled as two sequential respiratory mucosal stacks (anterior and posterior). The same modeling structure is used for the rat and human nose. The surface area and volumes of the tissue stacks were anatomically defined and are provided by Teeguarden *et al.* (2008) for the nose or from the models of Yeh as described in McBride (1992) for the trachea. Tissue vapor diffusivity was estimated as described in Morris *et al.* (1993) and was based on diffusivity of ethanol in water (Martin *et al.*, 1983).

Each respiratory mucosal tissue stack (in both the URT and the trachea) consists of a superficial airway lumen compartment, a mucus compartment, two epithelial compartments, and two submucosal compartments (Fig. 1B). Blood perfuses the submucosal compartments only, and a venous equilibration assumption is used, e.g., the concentration of vapor in blood exiting each submucosal compartment is assumed to be identical to the concentration in the submucosal compartment itself. For the rat and human, an olfactory submucosal blood flow of 1 ml/min/g tissue is used as this assumption provided the best fit to uptake efficiencies of a variety of vapors (Morris *et al.*, 1993). A respiratory mucosal blood flow of 0.36 ml/min was used as this provided the optimal fit of the previously published acetone and ethanol URT uptake data for the Sprague-Dawley rat (Morris and Cavanagh, 1986). Blood flow was partitioned between each nasal respiratory mucosal stack on the basis of their relative surface areas. Human respiratory mucosal blood flows are provided in Teeguarden *et al.* (2008).

Tracheal surface areas for the human and rat were derived from the models of Yeh as described in McBride (1992). Tracheal blood flows were estimated assuming that 1% of the cardiac output perfuses the tracheobronchial tree with the fraction of that flow perfusing the trachea being equivalent to the fraction of the total tracheobronchial surface area that was occupied by the trachea (4.9 and 1.3%, respectively, for the rat and human).

For the rat model, each compartment was assumed to be of 10 μm depth; thus, the total depth of the respiratory mucosal stack was 50 μm. For the human, each compartment was assumed to be 20 μm deep, for a total depth of 100 μm (Mahmood *et al.* 2006; Mariassy, 1992; Van Winkle *et al.*, 2004). Olfactory tissue was modeled similarly except that the olfactory epithelial layer was modeled as four compartments to account for the increased depth of this mucosa (Morris *et al.*, 1993). Vapor was transferred between each tissue compartment by diffusion, modeled as described in Morris *et al.* (1993). In addition, vapor was allowed to be metabolized in each epithelial and submucosal (but not mucus) compartment via Michealis-Menten kinetics also as described by Morris *et al.* (1993). The cardiac output provided by Teeguarden *et al.* (2008) was used.

The *in vitro* metabolism rates obtained for diacetyl were used to estimate tissue V_{max} assuming that the specific activities reported in Table 1 equaled the V_{max} values for each tissue. A Km = 1.1mM was assumed (Nakagawa *et al.*, 2002). Since there are no data on the cellular distribution of diacetyl reductase, it was assumed to be uniformly distributed throughout the epithelial and submucosal compartments of each mucosa. Enzyme activity was apportioned between compartments based on relative surface areas, e.g., since the dorsal medial respiratory epithelium was assumed to account for 12% of the total nasal respiratory mucosa surface area, the V_{max} of this tissue stack was assumed to be 12% of the total V_{max} measured in the respiratory mucosal homogenates. A surface area basis was used to estimate human V_{max} values. The nasal respiratory-, olfactory-, and tracheal-specific activities obtained from the *in vitro* studies (Table 1) were divided by the respective surface areas of these tissues to obtain V_{max}/cm^2 values. These values were then multiplied by the respective surface areas in the human respiratory tract to provide the human estimates.

Airborne vapor was allowed to diffuse into the mucous lining layer in accordance with mass transport theory as devised by Frederick *et al.* (1998) and described most recently by Teeguarden *et al.* (2008). Identical air-phase mass transfer coefficients were used in these two studies (see Table 1; Teeguarden *et al.*, 2008), and these values are also used in the current model to calculate the overall mass transport coefficient. Air-phase mass transport

TABLE A1
Model Parameters

Flow parameters	Rat	Human
Cardiac output (ml/min)	110[a]	7500[b]
Nasal respiratory mucosal blood flow (ml/min)	0.36[c]	18.75[b]
Nasal olfactory mucosal blood flow (ml/min/g tissue)	1[a]	1[a]
Tracheal blood flow (ml/min)	0.54[d]	0.98[e]
Vapor-specific constants		
Mucus:air partition coefficient	550[f]	50[f]
Tissue diffusivity (cm^2/min)	2.6×10^{-4}	2.6×10^{-4}
Surface areas (cm^2)[g]		
Dorsal respiratory tissue compartment	0.78	13.5
Olfactory tissue compartment	6.75	20.0
Anterior ventral tissue compartment	2.86	83.3
Posterior ventral tissue compartment	2.86	83.3
Anterior tracheal tissue compartment	1.43	31.5
Posterior tracheal tissue compartment	1.43	31.5
Metabolism rates (nmol/min/compartment)[h]		
Each dorsal respiratory tissue compartment	6	158
Each olfactory tissue compartment	128	1030
Each anterior ventral tissue compartment	21	511
Each posterior ventral tissue compartment	21	511
Each anterior tracheal tissue compartment	16	674
Each posterior tracheal tissue compartment	16	674

[a]Morris *et al*. (1993).
[b]Teeguarden *et al*. (2008).
[d]Optimized to the acetone and ethanol URT extraction data of Morris and Cavanagh (1986).
[e]Calculated from cardiac output and tracheal surface areas (see text).
[f]The water:air partition coefficient determined in this study was used as a surrogate for the mucus:air partition coefficient and was assumed to be identical in both species.
[g]Calculated from data of Teeguarden *et al*. (2008) for rat or from the total human nasal surface area of 200 cm^2 assuming a 90:10 ratio of respiratory to olfactory mucosa (U.S. EPA, 1994).
[h]Compartmental metabolism rates were calculated assuming uniform distribution among epithelial and submucosal compartments and normalized for tissue each stack from the total metabolism rate of the nasal or tracheal samples based on surface area of that stack.

coefficients are not known for the human or rat trachea, and the overall mass transport coefficient for the rat and human was estimated by the approach provided as equation 31 by Condorelli and George (1999) using the correlation parameters derived for ethanol (Table 4 in Condorelli and George, 1999).

The mass balance equation for diacetyl in each airway lumen was identical to that described by Teeguarden *et al*. (2008):

$$V_l dC_l/dt = Q_a(C_{in} - C_l) - K_{lt}(C_l - C_t/H_{ta}),$$

where V_l is the volume of the airway lumen over each tissue stack, C_l and C_t are the vapor concentration in the airway lumen and mucus compartment, C_{in} is the vapor concentration in air entering the airway lumen, Q_a is airflow over the mucus compartment, H_{ta} is the air:mucus partition coefficient, and K_{lt} is the lumen-to-tissue overall mass transfer coefficient, calculated as described by Frederick *et al*. (1998) for the nasal compartment or Condorelli and George (1999) for the trachea.

The mass balance equation for diacetyl in an epithelial compartment is given by

$$V_t C_{e2}/dt = k_b^* V_t^* (C_{e1} - C_{e2}) + k_b^* V_t^* (C_{s1} - C_{e2}) - V_{max}[C_{e2}/(C_{e2} + Km)],$$

where V_t is the volume of the tissue compartment (all tissue compartments of a stack are of the same volume), k_b governs the diffusion between compartments (as described by Morris *et al*., 1993), C_{e1}, C_{e2}, and C_{s1} are the concentrations in the superficial and deep epithelial and superficial submucosal compartments, respectively (see Fig. 1B), and V_{maxe2} and Km are the Michealis-Menten constants.

As the Teeguarden *et al*. (2008) model for acetaldehyde, the current model did not include a first-order direct reactivity term under the assumption that the first-order reaction rates of diacetyl were not sufficiently high to strongly influence uptake. Even if it were assumed that diacetyl were as reactive as acrolein (first-order reaction constant of 3 per minute; Schroeter *et al*., 2008), the predicted uptake efficiencies would be altered by only ~1.1-fold from their original value (e.g., from 33 to 37% at 400 ml/min).